UvA-DARE (Digital Academic Repository)

The M31 population of supersoft sources

Kahabka, P.

[Link to publication](#)

The M31 population of supersoft sources

P. Kahabka

Astronomical Institute and Center for High Energy Astrophysics, University of Amsterdam, Kruislaan 403, 1098 SJ Amsterdam, The Netherlands

Abstract. The 1991 *ROSAT PSPC* M31 X-ray point source catalog has been screened in order to set up a sample of candidate supersoft sources in this galaxy, additional to the 16 supersoft sources already known in M31 (Supper et al. 1997). Selection criteria used were based on hardness ratios ("X-ray colors"), as developed in an earlier paper (Kahabka 1998). An additional criterion to be fulfilled was that the observed count rate is in agreement with the expected steady-state luminosity for a source with these hardness ratios. This condition constrained mainly the hydrogen absorbing column towards the source. 26 candidates not correlating with foreground stars and M31 supernova remnants have been found to fulfil one of the selection criteria. They can be considered to be candidate supersoft sources in M31. This comprises 6% of all point sources in this galaxy. For these candidates absorbing hydrogen column densities, effective temperatures and white dwarf masses (assuming the sources are on the stability line of surface nuclear burning) are derived. An observed white dwarf mass distribution is derived which indicates that the masses are constrained to $M \gtrsim 0.90\ M_\odot$.

The entire population of supersoft sources in M31 is estimated taking a theoretical white dwarf mass distribution into account and under the assumption that the observationally derived sample is restricted to white dwarf masses above 0.90 $M_\odot$. Taking into account that the gas and the source population have different scale heights a total number of at least 200-500 and at most 6,000-15,000 sources is deduced (depending on the used galaxy N_H model), making use of the population synthesis calculation of Yungelson (1996).

The spatial distribution favors a disk (or spiral-arm) dominated young stellar population with a ratio of 1/(4-7) of bulge/disk systems, very similar to what has been found for novae in the Milky Way but lower than favored for novae in M31 ($\sim$1/2). Supersoft sources and Cepheids both show association with the M31 spiral arms and may belong to a younger stellar population. A mean space density of $\sim (0.1-5) \times 10^{-8}$ pc^{-3} is inferred for the supersoft sources. Assuming that all supersoft sources with masses in excess of 0.5 $M_\odot$ are progenitors of supernovae of type Ia, a SN Ia rate of $(0.8 - 7) \times 10^{-3}$ yr^{-1} is derived for M31 based on these progenitors. Supersoft sources might be able to account for 20-100% of the total SN Ia rate in a galaxy like M31.

Key words: galaxies:individual:M 31 – binaries:close – X-rays:stars – stars:evolution – white dwarfs

1. Introduction

Supersoft sources constitute an interesting new class of X-ray binary sources (cf. van den Heuvel et al. 1992). This is due to the fact that their spectra are extremely soft (effective temperatures of a few 10^5 K) and their luminosities are substantial ($10^{36} - 10^{38}$ erg s^{-1}). They thus can not only be studied in the Milky Way and the near-by Magellanic Clouds (LMC and SMC) but also in more distant galaxies (the Andromeda galaxy M31 and the spiral galaxy NGC 55). For a review see Hasinger (1994), Kahabka & Trümper (1996) and Kahabka & van den Heuvel (1997), see also Greiner (1996). They are considered to be at least one class of progenitors of type Ia supernovae (cf. Branch et al.1995, Livio 1996, Li & van den Heuvel 1997, Yungelson & Livio 1998, and Branch 1998).

In this article the observed sample of supersoft sources in the Andromeda galaxy (M31) is studied. A distance of 700 kpc is adopted (slightly different distances of 690 and 725 kpc are used in other literature). The inclination of the galaxy is 77.5^o. The inner "apparent bulge" has a radius of 3 kpc and the bulge is truncated at a radius of 6.4 kpc. The disk extends to a radius of $\sim$20 kpc (Hatano et al. 1997). First a number of candidate supersoft sources in M31 is derived from the 1991 X-ray point source catalog (retrieved from CDS via anonymous ftp 130.79.128.5) making use of the hardness ratios ("X-ray colors") HR1, HR2 and the count rate information.

For the 26 candidates a hydrogen column (N_H) distribution and a white dwarf mass distribution is derived assuming non-LTE white dwarf atmosphere spectra. The observationally derived white dwarf mass distribution is

compared with the mass distribution predicted from population synthesis calculations and the number of the population is corrected accordingly. The observationally derived N_{H} distribution is compared with a galaxy scale height N_{H} distribution and the population is corrected accordingly. This allows to constrain the whole active population distributed over the whole galaxy. Assuming objects with masses $> 0.8\ M_{\odot}$ (and $> 0.5\ M_{\odot}$ respectively) contribute as progenitors of type Ia SNe and explode after an evolutionary time scale of $\sim 10^{6}\ yr$ a SN Ia rate is derived for M31 from this population. This rate is compared with the total M31 SN Ia rate.

2. The sample of supersoft sources in M31

2.1. The SW-sample

15 firm candidate supersoft sources have been found in the 1991 *ROSAT PSPC* observations of M31 by Supper et al. (1997), cf. Greiner, Supper & Magnier (1997) by applying to the *ROSAT PSPC* hardness ratio HR1 which is defined as

$$\mathrm{HR1} = (\mathrm{H} - \mathrm{S})/(\mathrm{H} + \mathrm{S}) \tag{1}$$

with S = counts in channel 11-41 (roughly 0.1-0.4 keV), H = counts in channel 52-201 (roughly 0.5-2.1 keV). The selection criterion for a supersoft source is:

$$\mathrm{HR1} + \sigma \mathrm{HR1} \leq -0.80 \tag{2}$$

A 16-th supersoft source, a recurrent transient has been discovered by White et al. (1994). We call this subsample of 16 sources the Supper-White (SW) sample.

It has been shown by Kahabka (1998) that the individual spectral parameters giving information on the white dwarf masses of these 16 M31 supersoft sources can be constrained if the *ROSAT PSPC* hardness ratios HR1 and HR2 and the count rate as given in the catalog of Supper et al. (1997) are taken into account. The definition of HR2 is

$$\mathrm{HR2} = (\mathrm{H2} - \mathrm{H1})/(\mathrm{H2} + \mathrm{H1}) \tag{3}$$

with H1 = counts in channel 52-90 (roughly 0.5-0.9 keV), H2 = counts in channel 91-201 (roughly 0.9-2.0 keV). The hardness ratios HR1 and HR2 and the count rates have been compared with theoretical values derived using non-LTE white dwarf atmosphere spectra. As a result we found that for all these 16 sources the white dwarf masses were quite large $> 0.9\ M_{\odot}$.

In the present work non-LTE models of white dwarf atmospheres are used (Hartmann, private communication) extending to effective temperatures as low as $3 \times 10^{5}\ K$. Absorbing hydrogen columns N_{H} and effective temperatures T_{eff} have been determined in a N_{H}-T_{eff} plane from the overlap of the 90% confidence parameter regions as determined from the HR1, HR2 and count

rate constraints in that plane. In order to calculate the HR1-effective temperature planes somewhat reduced errors ($0.85 \times 1\sigma$ errors) have been used. This has the effect of bounding the hydrogen column to $N_{\mathrm{H}} > 8. \times 10^{20}\ \mathrm{H - atoms\ cm^{-2}}$ which is consistent with a minimum $N_{\mathrm{H}} \sim 6. \times 10^{20}\ \mathrm{H - atoms\ cm^{-2}}$ due to the galactic foreground column. In Table 1 values are given for the SW-sample taking these new constraints into account. These values differ only slightly from those derived in Kahabka (1998). Count rates are given for the broad (0.1-2.4 keV) band. It should be noted that although the standard deviations for some sources are very large (which might suggest that these sources are not detected significantly) all these sources have been detected significantly in the soft (0.1-0.4 keV) band (see Table 5 of Supper et al. 1997). The high standard deviations in the 0.1-2.4 keV band are due to the fact that in this band most of the counts are background ones from the 0.4-2.4 keV range.

White dwarf masses are determined under the assumption that the source is on the stability line of surface hydrogen burning (cf. Iben 1982). The source may even be on the plateau of the Hertzsprung-Russell diagram with radius expansion. Then its mass would be even larger. This method has been applied to the *Beppo-SAX* observation of CAL87 and CAL83 and reasonable white dwarf masses of $\approx 1.2\ M_{\odot}$ and $\approx 0.9-1.0\ M_{\odot}$ have been derived respectively (Parmar et al. 1997, 1998).

2.2. The complimentary sample (C-sample)

The SW sample cannot be complete as it has been shown that supersoft sources are expected to cover a much wider range in HR1 (Kahabka 1998). Actually all values of HR1 in the range $-1.0 \leq HR1 \lesssim +0.8$ are possible in case the hottest (most massive) and more strongly absorbed ($N_{\mathrm{H}} \leq 5. \times 10^{21}\ \mathrm{cm^{-2}}$) sources are included. Sources lying deep inside the galaxy disk or even located below the galaxy disk are expected to be at least in part even more strongly absorbed and are not covered by the selection criterion used for the SW sample. It may well be that part of this population is detectable but in order to investigate this point the calculations of model atmosphere spectra have to be extended to N_{H} values in excess of the present upper bound of $5. \times 10^{21}\ \mathrm{cm^{-2}}$.

The SW-sample per definition has no correlation with either a foreground star nor a supernova remnant. We define a complementary sample (the C-sample) as the sample covering a much wider range of candidates fulfilling the conditions:

$$\begin{array}{l} \mathrm{HR1} < 0.9 \\ \mathrm{HR2} + \sigma \mathrm{HR2} < -0.1 \\ \mathrm{exclude\ HR1} + \sigma \mathrm{HR1} < -0.8 \end{array} \tag{4}$$

The C-sample comprises 26 objects and is given in Table 1. It turns out to contain 4 objects correlating with foreground stars and 4 with supernova remnants. If all

Table 1. *ROSAT PSPC* count rates (0.1-2.4 keV), hardness ratios HR1, from non-LTE white dwarf atmosphere models M4 and M5 derived absorbing hydrogen columns (10^{21} cm^{-2}), effective temperatures $T_{\rm eff}$ (10^5 K), white dwarf masses $M_{\rm WD}$ ($M_\odot$), index and tentative identification from the Supper (1997) catalog (a = foreground star, e = SNR, * = bulge source).

	Source name	rate (10^{-3} s^{-1})	HR1	HR2	$N_{\rm H}$ (10^{21} cm^{-2})	$T_{\rm eff}$ (10^5 K)	$M_{\rm WD}$ ($M_\odot$)	Supper Cat./Id.	Remark
				the SW-sample					
SWa	RX J0037.4+4015	0.31±0.31	-0.93±0.31	0.02±0.71	1.4-1.7	3.7-4.3	0.92-0.98	3	[3,H]
SWb	RX J0038.5+4014	0.80±0.28	-0.92±0.08	-0.49±0.53	1.2-1.8	3.7-4.5	0.92-1.00	12	[1,H]
SWc	RX J0038.6+4020	1.73±0.29	-0.93±0.06	0.32±0.66	1.1-1.4	4.0-4.6	0.96-1.02	18	[3,H]
SWd	RX J0039.6+4054	0.44±0.44	-0.92±0.02	-0.04±0.71	1.3-1.6	3.9-4.4	0.94-0.99	39	[2,H]
SWe	RX J0040.4+4009	0.85±0.32	-0.94±0.06	-0.90±0.10	1.2-1.6	3.6-4.4	0.94-0.99	78	[1,H]
SWf	RX J0040.7+4015	1.26±0.32	-0.94±0.06	-0.31±0.64	1.1-1.5	3.7-4.5	0.92-1.00	88	[2,H]
SWg	RX J0041.5+4040	0.32±0.18	-0.95±0.05	-0.62±0.44	1.4-1.9	3.4-4.1	0.90-0.96	114	[1,H]
SWh	RX J0041.8+4059	0.49±0.24	-0.93±0.07	-0.63±0.43	1.3-1.9	3.6-4.4	0.92-0.99	128	[1,H]
SWi	RX J0042.4+4044	1.69±0.32	-0.93±0.07	-0.07±0.70	1.0-1.4	3.8-4.6	0.94-1.02	171	[2,H]
SWj	RX J0043.5+4207	2.15±0.55	-0.92±0.08	-0.27±0.66	1.0-1.4	3.9-4.8	0.95-1.03	245	[1,H]
SWk	RX J0044.0+4118	2.46±0.42	-0.94±0.06	0.11±0.81	0.9-1.3	3.9-4.7	0.95-1.02	268	[3,H]
SWl	RX J0045.5+4206	3.14±0.34	-0.89±0.07	-0.29±0.65	1.0-1.3	4.4-4.9	0.99-1.04	309	[2,H]
SWm	RX J0046.2+4144	2.15±0.39	-0.93±0.07	0.62±0.40	1.2-1.7	3.8-4.7	0.94-1.02	335	[2,H]
SWn	RX J0046.2+4138	1.12±0.40	-0.91±0.09	-0.27±0.65	1.0-1.4	3.8-4.7	0.94-1.02	341	[2,H]
SWo	RX J0047.6+4205	1.05±0.36	-0.92±0.07	0.06±0.70	≤1.6	≤4.0	≤1.03	376	[3]
SWt	RX J0045.4+4154	29.6±1.0	+0.78±0.03	-0.59±0.03	4.0-4.2	8.4-8.5	1.26-1.27		[2,H]
			complimentary sample to the SW-sample (C-sample)						
C17	RX J0039.7+4030	2.03±0.30	-0.85±0.10	-0.83±0.53	1.2-1.6	4.4-4.9	0.99-1.04	45	[1,H]
C18	RX J0047.0+4201	0.90±0.33	-0.84±0.22	-0.73±0.30	0.8-2.1	3.2-4.6	0.87-1.01	358/a	[1]
C19	RX J0043.9+5148	1.29±0.36	-0.38±0.24	-0.87±0.40	1.8-3.4	4.6-5.3	1.01-1.06	259	[1,H]
C20	RX J0040.5+4034	1.30±0.30	-0.37±0.23	-0.68±0.29	1.8-3.4	4.6-5.3	1.01-1.06	82/a	[1]
C21	RX J0041.8+4015	3.18±0.58	-0.35±0.14	-0.63±0.27	1.7-2.2	5.0-5.4	1.04-1.07	129	[2,H]
C22	RX J0047.0+4157	1.79±0.43	-0.14±0.24	-0.77±0.22	2.2-4.0	5.0-5.9	1.04-1.11	356/a	[1,H]
C23	RX J0039.4+4050	2.93±0.36	-0.05±0.12	-0.36±0.16	2.6-3.3	5.5-5.9	1.08-1.11	35	[2,H]
C24	RX J0044.4+4200	1.17±0.31	0.16±0.30	-0.58±0.24	3.5-5.4	5.3-6.5	1.06-1.15	280	[2,H]
C25	RX J0043.7+4127	1.12±0.32	0.21±0.40	-0.44±0.33	3.2-7.0	5.2-7.0	1.11-1.21	252	[2,H]
C26	RX J0042.8+4115	40.14±1.06	0.28±0.02	-0.18±0.03	1.4-1.5	7.4-7.5	1.21-1.22	208/*	[2,H]
C27	RX J0040.0+4100	2.04±0.32	0.33±0.17	-0.27±0.17	4.1-5.2	6.1-6.7	1.12-1.17	58	[2,H]
C28	RX J0042.2+4048	0.58±0.24	0.36±0.50	-0.72±0.45	4.0-10	4.5-7.2	1.10-1.20	156	[1]
C29	RX J0046.3+4238	3.10±0.64	0.37±0.24	-0.32±0.20	3.4-6.0	6.1-7.2	1.12-1.20	342	[2,H]
C30	RX J0045.4+4219	1.19±0.33	0.39±0.32	-0.52±0.28	4.6-5.8	5.9-6.9	1.11-1.18	307	[2,H]
C31	RX J0043.4+4118	6.86±0.62	0.48±0.08	-0.36±0.09	3.6-4.2	6.9-7.2	1.18-1.20	240/e	[3]
C32	RX J0043.3+4120	6.74±0.62	0.49±0.08	-0.64±0.09	3.8-4.4	6.9-7.2	1.18-1.20	235	[2,H]
C33	RX J0045.2+4136	2.44±0.45	0.49±0.24	-0.41±0.19	4.2-6.4	6.3-7.4	1.14-1.21	297/e	[2]
C34	RX J0039.7+4039	0.87±0.23	0.50±0.35	-0.65±0.23	>4.8	>5.9	>1.11	44/a	[1]
C35	RX J0046.1+4136	0.25±0.25	0.51±0.48	-0.74±0.27	>3.0	>6.0	>1.12	330	[1]
C36	RX J0043.6+4126	2.40±0.38	0.55±0.20	-0.77±0.13	4.5-6.7	6.5-7.5	1.15-1.21	249/e	[1]
C37	RX J0040.1+4021	0.46±0.19	0.62±0.33	-0.78±0.28	>6.8	>6.0	>1.12	62	[1]
C38	RX J0042.6+4043	1.55±0.31	0.63±0.22	-0.97±0.18	>5.6	>6.4	>1.14	185	[1]
C39	RX J0042.9+4059	0.90±0.28	0.64±0.31	-0.71±0.25	>5.3	>6.3	>1.14	212/e	[1]
C40	RX J0047.6+4132	0.32±0.32	0.75±0.26	-0.85±0.70	>4.4	>7.0	>1.19	374	[1]
C41	RX J0042.6+4159	1.75±0.82	0.85±0.14	-0.68±0.25	>4.4	>7.4	>1.21	183	[1]
C42	RX J0044.2+4026	0.07±0.07	0.89±0.13	-0.84±0.16	>5.0	>8.0	>1.24	271	[1]

Remarks: quality flag [1] = full overlap of HR1, HR2, CPS contours, [2] = medium overlap of HR1 and CPS contours and overlap of HR2 contours considering $3 - \sigma$ uncertainties, [3] = full overlap of HR1 and CPS contours but no overlap of HR2 contour possibly due to source confusion in the hard band for the SW-sample of supersoft sources in M31 (Supper et al. 1997, White et al. 1994, cf. Greiner, Magnier & Hasinger 1997) and for the C-sample, [H] = histogram flag, entry in $N_{\rm H}$-histogram, sources identified as (a) or (e) have no entry in the black histogram, index and tentative identification from the Supper (1997) catalog (a = foreground star, e = SNR, * = bulge source).

identifications are correct then this sample reduces to 18 objects. We introduce quality flags (1=high, 2=medium and 3=low) to qualify the overlap of the HR1, HR2 and count rate constraints in the $T_{\mathrm{eff}} - N_{\mathrm{H}}$-plane. "high" means that all three contours overlap, "medium" means that the HR1 and the count rate contour overlap and the HR2 contour overlap within 3-σ, "low" means that the HR1 and the count rate contour overlap and the HR2 contour does not overlaps within 3-σ. Especially objects C31 and C33 which have quality flags L and M respectively and correlate with SNRs may be discarded. Object C36 shows the characteristics of a perfect candidate (all the H1, H2 and CPS contours overlap) and a correlation with a SNR may be by chance. C18, C20, C22 and C34 correlate with foreground stars but show contour overlap. If they are indeed stars then their temperatures must be very low (possibly M stars).

A discussion of the individual candidate sources of the C-sample is beyond the scope of this article. Interestingly source C26 is located in the bulge of M31 and (if the classification is correct) could harbor a very massive white dwarf very similar to the SWt transient (cf. Table 1). This source may be recurrent or/and very luminous. The latter point is confirmed by the high detected count rate of $(40 \pm 1)\ 10^{-3}\ \mathrm{s}^{-1}$ (cf. the SWt transient has a very similar count rate of $(30 \pm 1)\ 10^{-3}\ \mathrm{s}^{-1}$).

3. Estimating the total population

In the work of DiStefano & Rappaport (1994) a population of supersoft sources has been derived e.g. for the M31 galaxy by making certain assumptions about their spatial distribution, temperature and luminosity distribution. Here the work of DiStefano & Rappaport can be significantly extended as the sample derived from the observations has been enlarged significantly and a white dwarf mass distribution and a hydrogen column density distribution is derived for this sample.

3.1. The observation derived N_{H} distribution

In Figure 1 the N_{H} distribution of supersoft sources from Table 1 with well determined N_{H} values is shown as a histogram. Each source is distributed with fractional numbers into a number of N_{H} bins determined by the uncertainty of the value of N_{H} given in Table 1. Errors for these fractional numbers have been calculated in the following way. Distribution of the same fractional numbers in a range of bins which is twice as large (twice the error) reduces the fractional number per bin by a factor of 2. Therefore we used $0.5 \times$ the fractional value per bin as the error per bin. Two histograms are given. The white histogram comprises all sources (i.e. 32) for which the N_{H} could be constrained reasonably well, the black histogram comprises objects (i.e. 26) not coinciding with foreground stars or M31 supernova remnants. The fact that for a com-

paratively large sample of 26 objects hydrogen column densities can be inferred allows to probe their spatial distribution in the galaxy disk assuming a simple scale height law like an exponential law. This method allows not only to probe their distribution but also to derive a mean scale height of the detectable population. It might well be required to extend this analysis to much larger N_{H} values in excess of $5. \times 10^{21}\ \mathrm{cm}^{-2}$ in order to cover the more deeply embedded objects. We extended our calculations to absorbing column densities as high as $1.1\ 10^{22}\ \mathrm{cm}^{-2}$ and applied them e.g. to the source with the catalog index 156 (cf. Table 1). We find that this source is consistent to be highly absorbed ($N_{\mathrm{H}} \sim 4 - 10\ 10^{21}\mathrm{cm}^{-2}$), the total N_{H} column density of the M31 disk at that location is $\sim 5.6\ 10^{21}\mathrm{cm}^{-2}$.
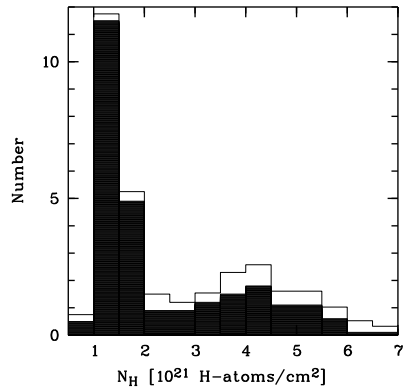

Fig. 1. Distribution of hydrogen absorbing column density for the M31 supersoft sources derived for 32 objects (white histogram) and 26 objects (excluding objects identified with foreground stars and SNRs, black histogram) from the sample in Table 1.

3.2. The derived white dwarf mass distribution

Deriving a mass distribution of a galaxy population is by far not trivial. In case of white dwarfs in supersoft sources it appears to be possible to derive reliable estimates of the masses using certain assumptions which have to be shown in later work to be correct or at least not completely unreasonable (cf. discussion in Kahabka 1998). From the numbers in Table 1 a mass distribution has been set up (cf. Figure 2). Each source is distributed with fractional numbers into a number of M_{WD} bins determined by the uncertainty of the value of M_{WD} given in Table 1. The histogram comprises all objects (i.e. 26) not coinciding with foreground stars or M31 supernova remnants for which the mass M_{WD} could be constrained reasonably well. The figure shows that only objects with masses in excess of $\approx 0.90\ M_{\odot}$ can be detected which is in agreement with the expected detection limit in *ROSAT PSPC* count rates

for the used exposure time of the observations (cf. Kahabka 1998). The reason is simply that for lower white dwarf masses the X-ray luminosities ate too low to be detectable.
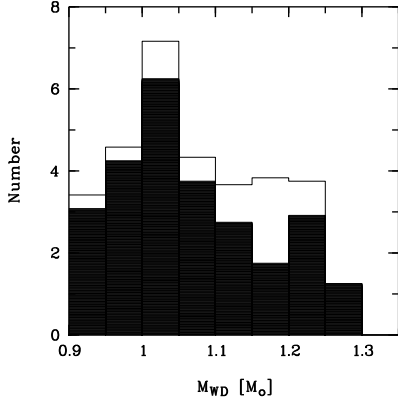
the first approximation appears somewhat small for the M31 galaxy.

Fig. 2. White dwarf mass distribution of the M31 supersoft sources derived for 32 objects (white histogram) and for 26 objects, excluding objects identified with foreground stars and SNRs (black histogram). The sample is taken from Table 1.

In Figure 3 the cumulative number distribution of white dwarfs in supersoft sources with masses $M > 0.5 M_\odot$ is given as deduced for the Milky Way in the calculations of Yungelson et al. (1996) for the t_{3bol}- and the hydrogen-burning shell approximation. t_{3bol} is the time it takes the white dwarf to decline by 3 magnitudes in its bolometric luminosity. Four distributions of supersoft sources are given for each approximation, the distribution of the CV class, the subgiant, symbiotic class and the total distribution. The total distributions have been used in our further discussion, e.g. to derive from the observed white dwarf distribution the predicted total distribution. In the t_{3bol} approximation 113 (out of 1895) objects are expected to be seen in the Milky Way with white dwarf masses in excess of 0.90 $M_\odot$ after correction for the limited visibility due to the N_H constraint and about 226 and objects in the twice as large M31 galaxy (see section 3.3). In the hydrogen-burning shell approximation 107 (out of 1553) objects are expected to be seen in the Milky Way with white dwarf masses in excess of 0.90 $M_\odot$ after correction for the limited visibility due to the N_H constraint and about 214 objects in the twice as large M31 galaxy. If one assumes that one is complete for masses in excess of 1.2 $M_\odot$ then the observed number of 4 systems (cf. Figure 2) would give a total population of $\sim$500 in the t_{3bol} approximation and a total population of $\sim$2000 in the hydrogen-burning shell approximation (as 16 for a population of 1895 are predicted in the t_{tbol} and 3.3 for a population of 1553 in the hydrogen-burning shell approximation). The number of the total population deduced from
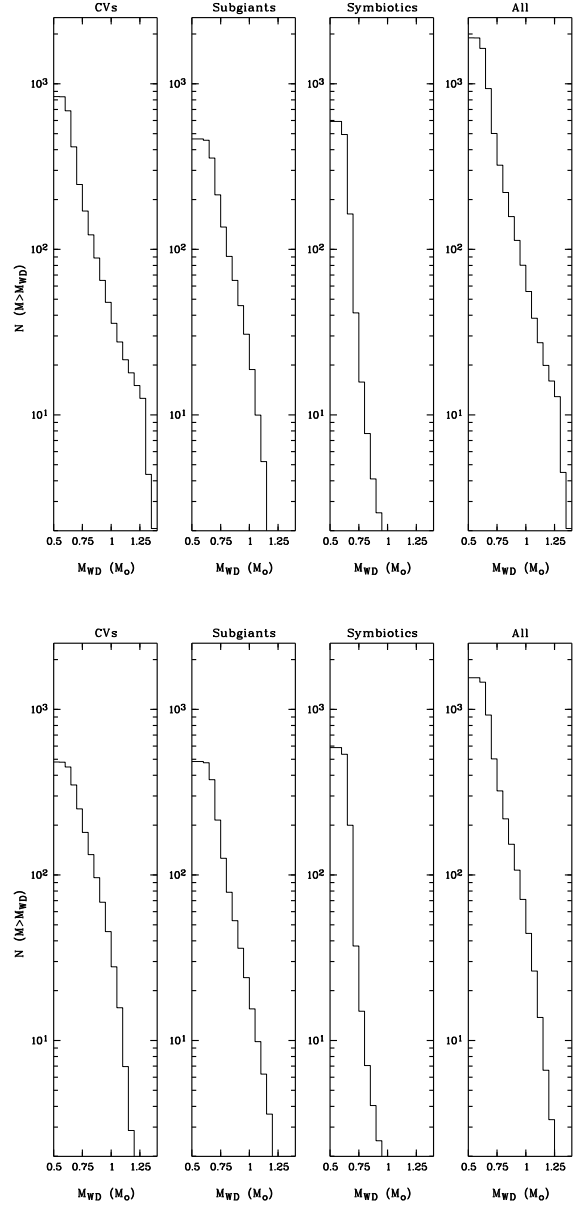

Fig. 3. Cumulative number distribution of CV-type, subgiant, symbiotic and total SSS for the Milky Way galaxy. Upper panel: t_{3bol} approximation, lower panel: hydrogen-burning shell approximation (deduced from Yungelson et al. 1996).

3.3. Correcting for the N_H and M_{WD} distribution

Using the observationally derived N_H and M_{WD} distribution one can, by comparing with the predicted distributions infer a total number of the population.

In a simple approach a double exponential description as e.g. introduced in DiStefano & Rappaport (1994) can be used to describe the source and the N_H distribution. The scale height of the source distribution h_s is assumed to be different from the scale height of the N_H distribution h_{nh}. Expressing the density distribution of the gas and hence the N_H distribution as

$$N_H = \int_z^\infty \rho dz = N_H^0 e^{-\frac{z}{h_{nh}}}, \tag{5}$$

where z is the distance from the galaxy plane, ρ the gas density, and N_H^0 the gas (roughly the hydrogen) column density at the base of the galaxy disk and expressing the source distribution as

$$dN_s = -\frac{N_s^0}{h_s} e^{-\frac{z}{h_s}} dz, \tag{6}$$

with N_s^0 the integrated (total) number of sources in the upper hemisphere of the galaxy disk (half of the total population) and h_s the exponential scale height of the source population, then one gets from Equation 5

$$z(N_H) = -h_{nh} \ln(N_H(z)/N_H^0). \tag{7}$$

Then Equation 6 can be reduced to

$$dN_s = N_s^0 \frac{h_{nh}}{h_s} (N_H(z)/N_H^0)^{\frac{h_{nh}}{h_s}} \frac{d(N_H/N_H^0)}{(N_H/N_H^0)} \tag{8}$$

Setting

$$h = \frac{h_{nh}}{h_s} \tag{9}$$

and

$$n = (N_H/N_H^0) \tag{10}$$

then Equation 8 reduces to

$$dN_s = N_s^0 h n^{(h-1)} dn. \tag{11}$$

Equations 8 and 11 give the expected number of sources (above the galaxy disk) and within the normalized N_H interval $d(N_H/N_H^0)$. From the distribution of observed numbers per N_H interval the scale height ratio $\frac{h_{nh}}{h_s}$ can be derived (as well as the total number of the population N_s^0). This distribution has a powerlaw behavior with slope (h-1). If the slope of the source distribution equals the slope of the gas distribution then the scale height ratio is $h = \frac{h_{nh}}{h_s} = 1.0$. The scale height for the gas may be in the range 150-600 pc for the M31 galaxy (cf. Braun 1991).

4. Constraining the scale height ratio and the total population from the normalized N_H histogram

We now will derive from Equation 11 the total population of supersoft sources in M31 and the scale height of this population with respect to the scale height of the M31 gas. In a first step we define the models used for the M31 gas, in a second step we derive the scaled N_H distribution and in a third step we apply a least-square fit to the scaled N_H distribution.

4.1. Possible N_H-models

From Equation 8 follows that the scaled $n = (N_H/N_H^0)$ distribution has to be considered in order to derive the relative scale height of the source distribution and the total number of the population. We now discuss two possible models for the N_H-distribution: a schematic one by Supper (1997) and a detailed based on radio observations.

4.1.1. the Supper-N_H model

In a first approach we use the galaxy N_H model given in Figure 12 of Supper (1997). The galaxy is divided into 3 concentric ellipsoids covering the disk and one circle at the central bulge. The positions of the candidate supersoft sources have been projected onto the galaxy disk (cf. Figure 4). The disk of M31 may be warped and flaring at the outer part (cf. Evans et al. 1998). Such a warping and flaring of the M31 disk may affect the scale height assumptions of those supersoft sources which are found in annulus III of the N_H-model of Supper (1997). This point deserves further investigation (cf. the galactocentric dependence of a galaxy scale height given by Evans et al. 1998 for the M31 disk, cf. also Braun, 1991).

4.1.2. the Urwin-N_H model

As a more refined model for the N_H distribution in M31 the Urwin (1980) model is used. The radial distribution of the hydrogen column is calculated from the profile given in Figure 8 of Urwin (1980) making use of the equation given in Dickey & Lockman (1990)

$$N_H = 1.823 \times 10^{18} \int T_b \delta v \text{ cm}^{-2} \tag{12}$$

with the brightness temperature T_b, the integral is over the velocity profile. With an inclination of 77.5^o of the galaxy a maximum column density of $1.5 \ 10^{22} \text{ cm}^{-2}$ is derived for the NE HI profile and a maximum of $8.4 \ 10^{21} \text{ cm}^{-2}$ for the SW profile. The HI profile (not corrected for inclination) as determined from Equation 12 with $\int T_b \delta v$ taken from Figure 8 of Urwin (1980) is shown in Figure 5.

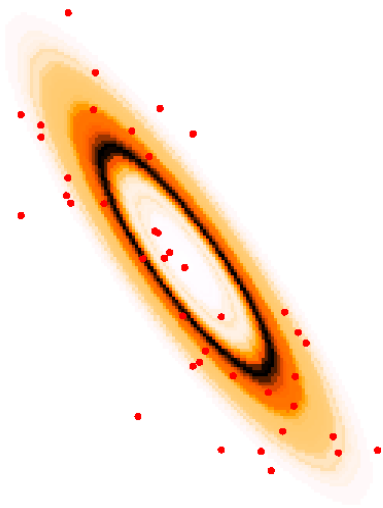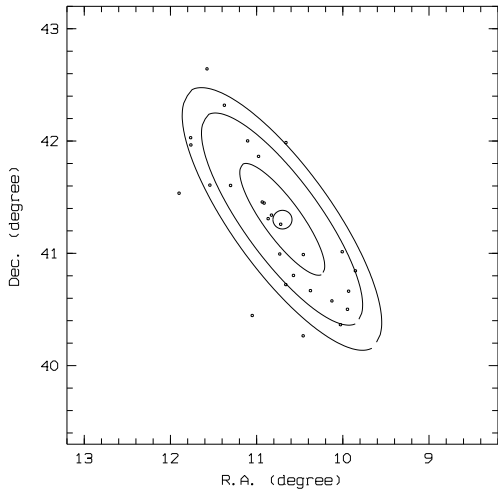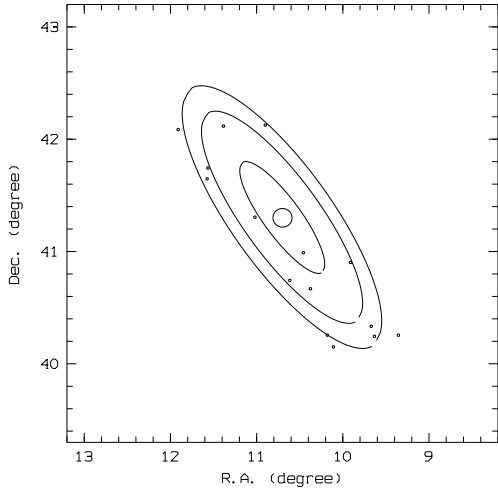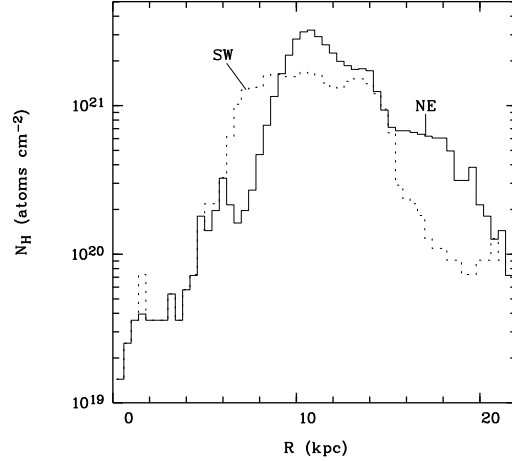**Fig. 5.** Radial hydrogen column density profile of M31 not corrected for the inclination of the galaxy. The solid histogram gives the north-eastern (NE) profile and dashed histogram gives the south-western (SW) histogram (calculated from the $\int T_b \delta v$ given in Figure 8 of Urwin (1980) and Equation 12).

We do not take molecular hydrogen into account. We just mention that a value of 4×10^{22} cm^{-2} has been measured at the location RA (1950) = $0^h 39^m.9$, Decl (1950) = $41^o 14'$ due to molecular hydrogen (cf. Urwin 1980, page 257).

4.2. Expected incompleteness of coverage as a function of hydrogen column density and white dwarf mass

In Kahabka (1998) the theoretically expected source count rate has been derived at the distance of M31 from non-LTE white dwarf atmosphere models (model M4) for white dwarf masses in the range $\sim 0.95 - 1.35$ $M_\odot$ under the assumption the source is on Iben's stability line of surface hydrogen burning (cf. Iben 1982). We extended these calculations (model M5) to white dwarf masses as low as 0.85 $M_\odot$ (cf. section 2.1). Taking the theoretical white dwarf mass distribution derived by Yungelson (1996) into account a number/count rate diagram was calculated as a function of the hydrogen column. The result is given for models M4 and M5 in Figure 6. From this diagram the completeness correction factor as a function of the hydrogen column has been derived making the following assumption. The X-ray survey of M31 by Supper (1997) is according to Fig. 13 of Supper complete for *ROSAT PSPC* count rates $\gtrsim 10^{-3}$ s^{-1}. From our Fig 6 the fractional number of sources seen for a specific hydrogen column assuming a cut-off count rate of 10^{-3} s^{-1} is derived. This fraction is equal to 1.0 for hydrogen columns $\lesssim 8.$ 10^{20} cm^{-2}. The inverse of this fraction has been used as the correction factor to derive the completeness corrected normalized N_H histogram making use of the specific galaxy N_H model.

Fig. 4. N_H model of M31 as taken from Supper (1997), Figure 12 for the SW-sample (upper panel) and C-sample (middle panel). Bottom: N_H image of M31 deduced from the radial profile of the HI intensity (Urwin 1980). The positions of the supersoft source candidates (the SW-sample and the C-sample) are given (lower panel).

Making e.g. use of the Supper galaxy N_{H} model it fol-
lows that for all annuli of the galaxy ellipse (including the
bulge) completeness is not guaranteed and the lower hemi-
sphere population is only partially seen. This agrees with
the rather small fraction of 0.22 of the total galaxy popu-
lation found for $n > 1$ i.e. at the other side of the midplane
of the disk of M31. From Figure 6 it becomes clear that for
$N_{\mathrm{H}} = 5. \times 10^{21}$ only candidates with masses $> 1.15 M_{\odot}$ are
detectable. This means adding the mean foreground N_{H} of
$6. \times 10^{20}$ in Supper's model annulus III is opaque for the
lower hemisphere population with $M_{\mathrm{WD}} \leq 1.15 M_{\odot}$ but
the bulge and annulus II are transparent for somewhat
less massive white dwarfs ($M_{\mathrm{WD}} \leq 1.05 M_{\odot}$).

Fig. 7. Fraction of sources with white dwarf masses above
$0.90 \ M_{\odot}$ seen in the Andromeda galaxy (M31) for differ-
ent hydrogen absorbing columns. This fraction is equal to
1.0 for columns below 8. 10^{20} cm^{-2}, which means com-
pleteness is fulfilled and decreases for increasing columns.

ing the completeness correction. The scaled N_{H} histogram
is plotted in Figure 8. This distribution extends from n=0
to n=2 and comprises both hemispheres of the galaxy. It
turns out that of the 18 sources in the distribution 22% (4
of 18) fall below the galaxy disk. This may not be unex-
pected as the masses and hence temperatures of the white
dwarfs involved are substantial and the total N_{H} of the
galaxy disk is only in one N_{H} ellipse large enough (i.e.
$\approx 7.7 \times 10^{21}$cm^{-2}) to hide the lower hemisphere popula-
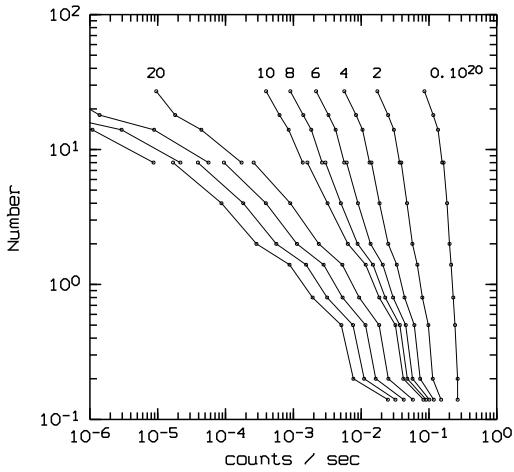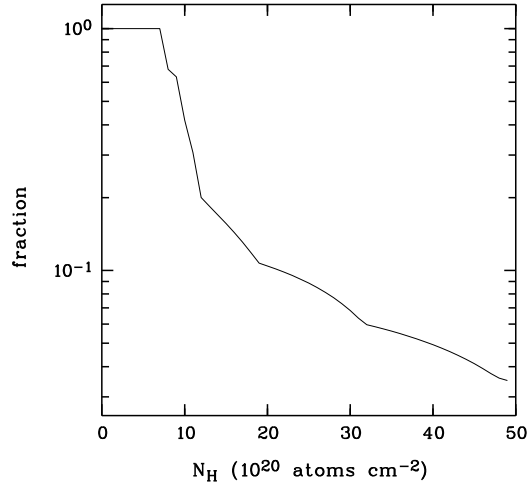tion nearly completely.

Fig. 6. Theoretical number/count rate diagram of super-
soft sources for a galaxy of the size of the Milky Way and
for a distance of 700 kpc (M31). Note that a galaxy like
M31 has a mass twice as large as the Milky Way. These
numbers follow from the population synthesis calculations
of Yungelson et al. (1996) for the Milky Way galaxy. La-
bels mark hydrogen column densities (10^{20} cm^{-2}). Dots
mark white dwarf masses (counted from bottom to top)
1.34,1.29,1.25,1.20,1.15,1.10,1.00(twice),0.95,0.90,0.85
$M_{\odot}$. This figure shows the results for model M5
($M_{\mathrm{WD}} \leq 1.0 M_{\odot}$) and for model M4 ($M_{\mathrm{WD}} \geq 1.0 M_{\odot}$).

Making use of the number/count rate distribution de-
rived from model M4 and M5 the fraction of objects seen
for different hydrogen columns has been calculated and the
result is given in Figure 7. This fraction is equal to 1.0 for
columns below 8.10^{20} cm^{-2}, which means completeness is
fulfilled, and decreases for increasing columns.

4.3. Number of supersoft sources expected for the Supper-N_{H} model

The scaled $n = (N_{\mathrm{H}}/N_{\mathrm{H}}^0)$ values have been derived mak-
ing use of the N_{H} ranges given in Table 1, deriving the
local N_{H}^0 values from the Supper N_{H} model and by apply-
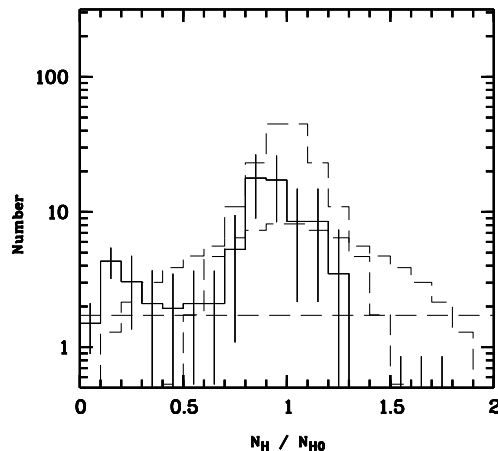

Fig. 8. Normalized $N_{\mathrm{H}}/N_{\mathrm{H}}^0$ distribution corrected for
completeness with 80 (corrected) candidates with well de-
termined N_{H} values in the n=0.0-1.0 interval. The best-fit
for a population of 1000, 2500, and 5000 sources is given
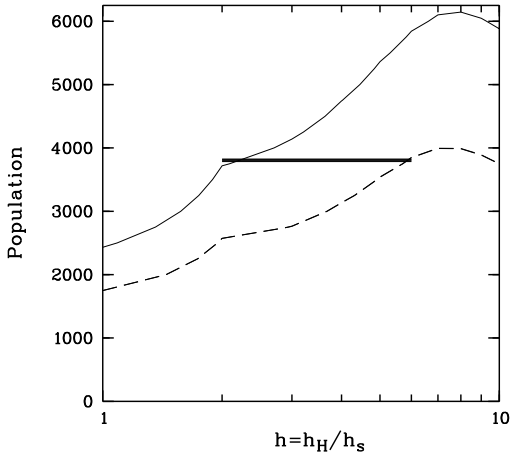as dashed histogram.

Fig. 9. Result of chi-squared fit (of Equation 11) to the distribution of Figure 8. The scale height ratio $h = h_H/h_s$-population plane is shown. The fit has been applied to the $0 < n < 1.0$ distribution (upper hemisphere). The 90% and 95% confidence bounds are shown as dashed and solid lines. The bar gives the estimate derived from the galactic population, cf. section 4.4

The total population can be inferred with Equation 11. Using the number of the corrected population above and below the galaxy disk of 80 (which is uncertain in the range 30-130 considering the errors, cf. Figure 8) and assuming that only a fraction of 6.0% of the whole population in the t_{3bol} and of 6.9% in the hydrogen-burning shell approximation is covered as only objects with white dwarf masses in excess of $0.90 M_\odot$ are detected a total population of 1300 (500-2200) and 1200 (430-1900) respectively is derived for the Andromeda galaxy. These numbers are consistent with the range of $\sim$800-5000 supersoft sources predicted from the population synthesis calculations of DiStefano & Rappaport (1994). The distribution would be consistent to be centered at $N_H/N_H^0 = 1$. This fits with a disk population of a scale height significantly smaller than the gas scale height. A scale height ratio can be constrained from this histogram. This means the scale height of the source distribution h_s can be determined with Equation 9 if the scale height of the gas distribution h_{nh} is known. As a function of galactocentric radius h_{nh} varies from 150 pc to 600 pc (Braun 1991). A chi-squared fit has been applied to the normalized N_H distribution. The result of a chi-squared fit of Equation 11 to the distribution given in Figure 8 is given in Figure 9. The range of the population follows from the chi-squared fit to the measured distribution taking the errors into account. A total population of 1,800-5,800 sources is obtained for h-values 1<h<6, which means for a source population which is more confined to the galaxy disk than the gas distribution. If there is a large population of supersoft sources in M31 then the sources are very confined to the galaxy plane. There may exist a number of the order 200 hot

($> 10^5$ K) and X-ray luminous planetary nebula nuclei in a spiral galaxy of the size of M31 according to the estimates of Iben & Tutukov (1985). They can be a minor sub-population of a larger population of luminous supersoft sources but with a larger scale height (h<1). From the formal fit of Equation 11 to the normalized N_H distribution (making use of the Supper-N_H model) we would exclude that a population of hot and luminous planetary nebula nuclei (of order of 200 objects) alone account for the observed sample.

4.4. Number of sources expected with the Urwin-N_H model

The normalized N_H histogram is also calculated by making use of the Urwin N_H model for the north-eastern (NE) part of the galaxy. This N_H model consists of a radial distribution with 57 rings. This distribution has been converted into a galaxy N_H model of M31 by assuming an inclination of the galaxy of 77.5^o (cf. Figure 4). This is a more refined model than the Supper-N_H model. The normalized distribution is given in Figure 10. This distribution appears to cover only parts of the normalized N_H-bins. The main histogram extends over the range $\frac{N_H}{N_{H0}}$=0.0-0.6. This fact can be explained if one considers the galactocentric distribution (12-16 kpc) of the sources which fall into this interval (cf. section 5) and the projected hydrogen columns of the M31 galaxy $\sim (4-9)\ 10^{21}$ cm^{-2} for these radii. The hydrogen columns are that large that indeed only part of the upper hemisphere population is detectable in agreement with the histogram extending to values well below n=1.0. The entries in the histogram for n$\sim 1.5 - 2.0$ are from the population found at radii 18-23 kpc. Here the projected hydrogen columns of $\sim (1 - 3)\ 10^{21}$ cm^{-2} are lower and the lower hemisphere population is detectable. But this part of the histogram is not very significant. We constrain our fit of Equation 11 only to the n=0.0-0.6 regime. This allows to constrain the size of the population and the scale height ratio. As we do not cover the top of the distribution we are not able to determine an upper bound for the population. Only by constraining the scale height ratio to realistic values for stellar populations we can determine an upper bound for the population.

The size of the population as derived with the Urwin-N_H model is consistent to be in the range $\sim$1000-10,000 sources for a scale height ratio h=1-5 (cf. Figure 11).

As a refined model the radial profiles of the north-eastern (NE) and the south-western (SW) galaxy as given in Urwin (1980) have been used to calculate a N_H-map of the galaxy and to deduce the hydrogen-column at the location of each supersoft source. The normalized N_H distribution has been calculated which is given in Figure 12. This distribution extends over a similar N_H/N_{H0} range as for the Urwin model. A fit of Equation 11 to this distribution for a population is given in Figure 13 as a func-
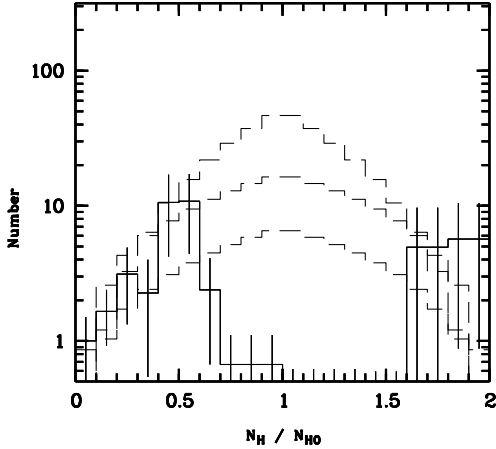
Fig. 10. Normalized N_H/N_H^0 distribution corrected for completeness with 24 (corrected) candidates with well determined N_H values in the n=0.0-0.6 interval. The best-fit for a population of 1000, 2500, and 5000 sources is given as drawn and dashed histograms.
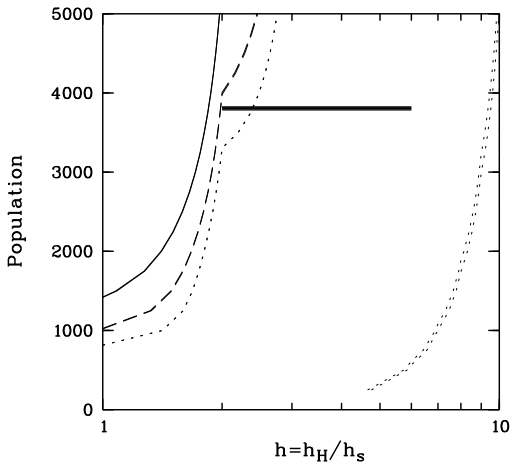

Fig. 11. Result of chi-squared fit (of Equation 11) to the distribution of Figure 10. The confidence plane for the scale height ratio $h = h_H/h_s$-population plane shown. The 95% confidence bound is given as solid line and the 90% confidence bound as dashed line. The 10% confidence is given by a dotted line. The fit has been applied to the $0 < n < 0.6$ distribution (part of upper hemisphere).

M31 supernova remnant. Another possibility is that these sources are located at a large distance from the galaxy plane (>500 pc) and are projected due to the considerable inclination of the galaxy towards the wrong reference hydrogen column. But this appears to be quite unlikely.
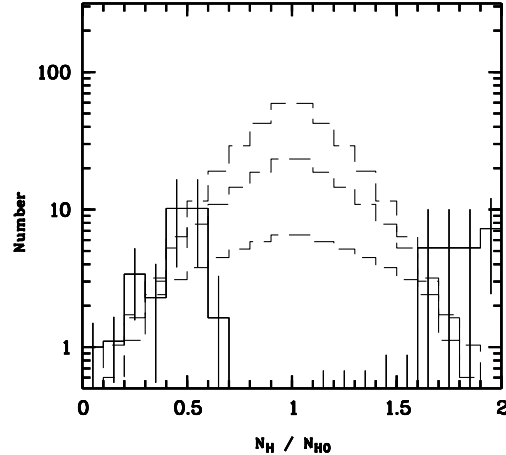

Fig. 12. Normalized N_H/N_H^0 distribution corrected for completeness with 23 (corrected) candidates with well determined N_H values deduced with the Urwin N_H model (NE and SW galaxy) in the $n = \frac{N_H}{N_{H_0}}$ interval n=0.0-0.6. The dashed histograms give the best-fit for a population of 1000, 2500, and 5000 sources.

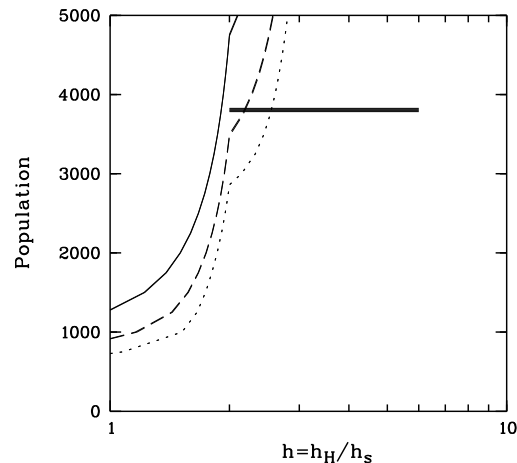**Fig. 13.** Result of chi-squared fit (of Equation 11) to the distribution of Figure 12. The scale height ratio $h = h_H/h_s$-population plane is shown. The 90% and 90% confidence bounds are shown as dashed and solid lines. The 10% confidence bound is shown as dotted line. The fit has been applied to $0 < n < 0.6$ distribution (part of upper hemisphere). The bar gives the estimate derived from the galactic population, cf. section 4.3.

tion of the scale height ratio $h = h_H/h_s$. This distribution again extends mainly over the n=0.0-0.6 interval (see discussion above). The size of the population is ~1000-10,000 for a scale height ratio h=1-5. There are sources from Table 1 which fall beyond the n=2 limit and are rejected (in the specific N_H-model). For the NE-SW Urwin model these sources are found either at radii >15 kpc or at radii <5 kpc. The nature of these sources is unclear or the N_H-model is still too crude (but see discussion in section 5). Some sources correlate with a foreground star or a

Table 2. Population of supersoft sources in M31 derived from a chi-square fit of Equation 11 to the normalized N_H histogram for different galaxy N_H models and different scale height ratios $h = \frac{h_{nh}}{h_s}$.

		population/1000		
N_H model	fit applied to	h=1	2	5
Supper	(0<n<1.0)	1.8-2.5	2.5-3.8	3.5-5.3
Urwin	(0<n<0.6)	<1.5	<5	<15
Urwin-NE-SW	(0<n<0.6)	0.5-1.3	2-5	5-15

The NE-SW model may describe the distribution of the hydrogen column in M31 in a good approximation. It becomes evident that in the range of galactocentric radii 12-16 kpc where most supersoft sources are found the hydrogen column is that large that only part of the upper hemisphere population is visible. The total population can be constrained dependent on the scale height ratio.

In Table 2 the size of the population of supersoft sources in M31 as derived from different galaxy N_H models is summarized. In the Supper N_H model numbers have been derived from the n=0-1 histogram (the complete upper galaxy hemisphere) and in the Urwin N_H model from the n=0-0.6 histogram (60% of the upper galaxy hemisphere). Interestingly the range of the population derived from different N_H models does not differ much. This may be due to the fact that the errors associated with the (corrected) numbers are substantial due to the small number of selected sources. In order to better confine the range of the population detections of supersoft sources in the 12-16 kpc ring for values n>0.6 are required. Such sources are heavily absorbed, they have hydrogen columns $N_H > 2.5 - 5 \ 10^{21} \ cm^{-2}$ according to Figure 6 and they are only detected in the *ROSAT* 1991 survey of Supper if the white dwarf mass is in excess of 1.2 $M_\odot$ (see possible candidates in the C-sample, cf. Table 1).

4.5. Comparison with the galactic population

There is evidence that the group of observed galactic supersoft sources is larger than assumed. Patterson (1998) proposes three sources to belong to this family, e.g. V Sge, T Pyx and (possibly) WX Cen. These blue and optically bright binary systems have orbital periods of 12, 2, and 10 hours. Assuming distances of 1.3, 2.5, and 1.4 kpc the objects are found 200, 430, and 16 pc above the galactic plane. The two "standard" galactic supersoft sources RX J0925.7-4758 and RX J0019.8+2156 are 33 and 840 pc above the galactic plane assuming distances of 1 kpc. Assuming an exponential z-distribution (cf. Equation 6) and assuming a scale height for the source population h_s the total population can be constrained in order to be consistent with this sample. This is an independent con-

sistency check for the distribution and size of the galactic sample. Assuming a scale height of 150 pc the population has to be greater than 270 in order to explain the discovery of one source such as RX J0019.8+2156 at such a large scale height. Assuming a much smaller scale height of 30 pc the probability of observing one RX J0019.8+2156 is negligible. The scale height of a population of supersoft sources which can explain RX J0019.8+2156 has to be larger than 105 pc if the total population is <3000. This is not a problem as 105 pc is still a small scale height for stellar populations. T Pyx is a recurrent supersoft source which is found 200 pc above the galactic plane. T Pyx may harbor a massive white dwarf as it has a recurrence period of 20 years. According to the population synthesis calculations of Yungelson (1996) there may be 113 galactic supersoft sources which are more massive than 0.9 $M_\odot$. These sources can become recurrent supersoft sources with such a recurrence period (cf. Kahabka 1995). Assuming a scale height of 105 pc for the source distribution 2 sources are expected to be found at a distance from the galactic plane as large as in T Pyx (430 pc). To observe one T Pyx is therefore in full agreement with this number. The distance from the galactic plane of all other supersoft sources is considerably smaller and is in agreement with such a population. The conclusion is that the prediction of a population of ~1900 supersoft sources in the Milky Way by the population synthesis calculations of Yungelson (1996) is in agreement with the so far discovered galactic population if the scale height is ~100 pc. One expects then 0.6 systems to be observed at the distance from the galactic plane of 840 pc, the distance of RX J0019.8+2156.

Assuming a scale height for the galactic supersoft sources of 100 pc and a scale height for the gas of 200-600 pc a value $h = 2 - 6$ (Equation 9) is derived. Scaling with the mass ratio of the Andromeda galaxy and the Milky Way galaxy, which is about 2, one expects from the population synthesis calculations of Yungelson (1996) that there exists a population of ~3800 supersoft sources in M31. Such a population having $h = 2 - 6$ is consistent with the chi-squared fit to the normalized N_H distribution given in Figure 9, 11 and 13. There is still the possibility of a bi-modal population consisting of a more extended population (e.g. the CV-type supersoft sources) and a more to the galaxy plane confined population (e.g. the subgiant class). We fitted such a bi-modal population to the normalized N_H histogram of Figure 12 and find that an extended $(3 > h > 1)$ population of 500 sources and a confined (h<10) population of ≤ 6000 sources is possible.

5. The spatial distribution

The 26 supersoft sources found in M31 are distributed over the whole galaxy disk (cf. Figure 4 for the distribution of the SW and the C-sample, cf. also Figure 14 and Figure 15). This may be in favor for a disk population. Recent spatial studies of novae in M31 using a Monte Carlo simu-

lation have been performed by Hatano et al. (1997). From this study it follows that the ratio of bulge to disk population is about 1/2 similar to the ratio of bulge to disk mass of this galaxy although there is some controversy about this subject. In comparison for the Milky Way a ratio of 1/7 is found both for the novae and the mass. The M31 bulge has in the model of Hatano a radius of ∼6 kpc (equivalent to a projected size of 0.5^o). A more extended discussion on the distribution of novae in M31 can e.g. be found in Capaccioli et al (1989), Rosino et al. (1998) and Yungelson et al. (1997). Interestingly there are 6 of the 31 (likely) candidate supersoft sources found in the bulge region. But three of these objects correlate eiher with a galactic foreground star or a M31 supernova remnant. A ratio 1/(5-10) is derived for supersoft sources detected in the bulge compared to objects detected in the disk. This ratio reduces to 1/(4-7) if only "accepted" systems are considered (cf. Figure 15). There may be a chaining of supersoft sources (from the C-sample) along a ∼(12-16) kpc arm (cf. Figure 4,5, 14 and 15). This feature may also be found in the model of Hatano (cf. his Figure 3). The spatial distribution of the SW-sample (with a mean radius of 14 kpc) is consistent with a 12-16 kpc spiral arm of the M31 galaxy (cf. Figure 6 of Braun 1991). Another grouping of supersoft sources in a 18-21 kpc ring (cf. Figure 15) may be connected to a 18-24 kpc spiral arm (cf. Braun 1991). There are no detections within the 6-12 kpc ring (the only exception may be the source with the catalog index 212). In this ring the (projected) hydrogen column reaches values up to 1.5×10^{22} cm^{-2}.
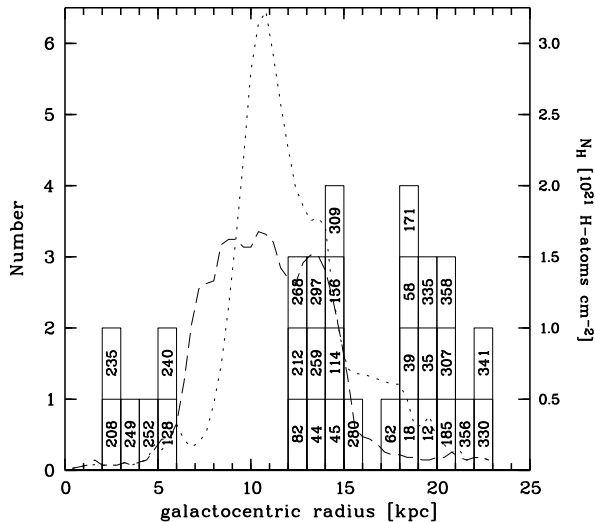

Fig. 14. Distribution of supersoft sources in M31 (solid histogram) as a function of the galactocentric distance in M31. Also shown is the radial distribution of the hydrogen column density for the NE Urwin model (dotted line) and for the SW Urwin model (dashed line) which is not corrected for the inclination of the galaxy. The catalog indices of individual sources are given (cf. Table 1).

In Figure 15 we also show the galactocentric distribution of the M31 novae (from Sharov & Alksnis 1991, 1992), blue stars (B-V<0.3) and Cepheids (from Magnier et al. 1992, 1997 and Haiman et al. 1994). Novae belong to an old stellar population and are preferentially detected in the bulge (at galactocentric radii ≲6 kpc). Blue stars belong to a young stellar population and trace the galaxy light. Cepheids belong to a somewhat older population. The distribution of Cepheids trace the spiral arms of M31 where recent star formation is taking place. They are found (in the distribution) predominantly within 8-15 kpc. For a consideration of the completeness of the Cepheid sample see Magnier et al. (1997). Actually there could be a second Cepheid peak at galactocentric radii 18-22 kpc where another M31 spiral arm is found and where a peak in the supersoft distribution is found. But the Magnier survey apparently did not cover this region.

While novae appear to be bulge-dominated in the observational sample most possibly due to the low dust content of the M31 bulge supersoft sources appear to be to a less degree bulge-dominated and are more likely associated with the spiral arms. Considering only objects with 0<n<2 then supersoft sources are found within galactocentric radii of 5-25 kpc. They are not found in the bulge of M31, but within the range of Cepheids and blue stars and at 18-22 kpc. Bulge sources at galactocentric radii r<6 kpc are only found in the "intrinsically absorbed" sample. They may be consistent with classical or symbiotic novae as these objects show high intrinsic absorption and tend to belong to an old population. The M31 supersoft sources may belong to a younger population similar to the Cepheids but to an older population than blue stars. Hatano et al. assume a scale height of the M31 novae of 350 pc. We find that the scale height of the M31 supersoft sources is consistent to be smaller (100-150 pc, at 5 kpc) which favors a younger stellar population and is in agreement with the supported view that slightly evolved main-sequence stars or subgiants are involved (van den Heuvel et al. 1992). A mean space density can be inferred for the population of supersoft sources in M31 (assuming that they are homogeneously distributed in a disk of radius 20 kpc and have a scale height of 150 pc) of ∼ $(0.1 - 5) \times^{-8}$ pc^{-3}. One could suspect from Figure 15 that we see two different sub-populations of supersoft sources, one in the bulge at galactocentric radii <6 kpc, possibly associated with (classical and symbiotic) novae, one at radii 12-16 kpc and 18-20 kpc respectively tracing spiral arms and possibly associated with subgiants and CV-type supersoft sources and one at radii 18-22 kpc also associated with a spiral arm and possibly associated with subgiants and CV-type supersoft sources.
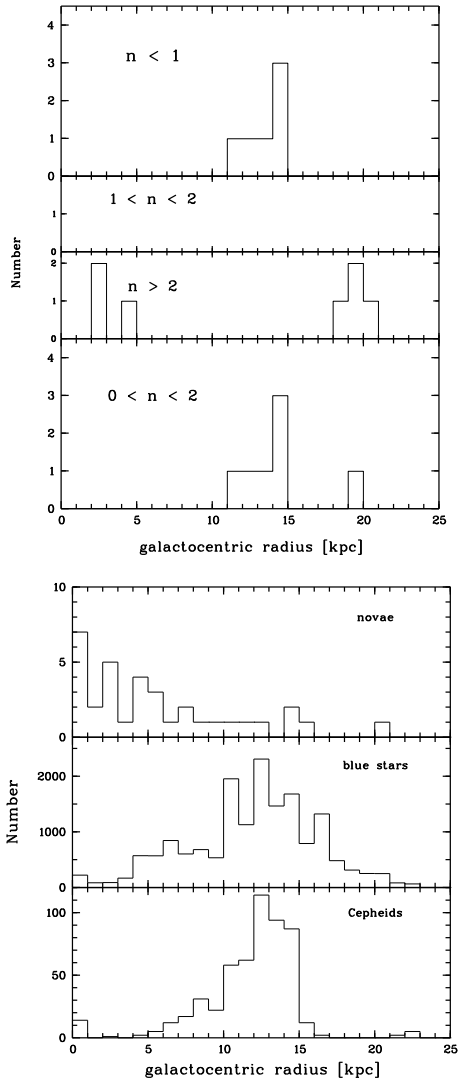
Fig. 15. Upper panel: galactocentric distribution of supersoft sources in M31. Separate histograms are shown for objects not correlating with a foreground star or a M31 supernova remnant and located in the upper (n<1), lower (n>1) galaxy hemisphere. Also the distribution of "intrinsically absorbed" sources (n>2) is shown and the distribution for both hemispheres (0<n<2). Lower panel: galactocentric distribution of novae (from Sharov & Alksnis 1991, 1992), M31 blue stars with B-V<0.3 (from Magnier et al. 1992 and Haiman et al. 1994) and Cepheids (the Baade and Magnier sample, cf. Magnier et al. 1997).

6. Estimating a SN Ia rate inferred from the population of supersoft sources in M31

Assuming a total number of ∼1000-10,000 active supersoft sources in M31 as follows from an analysis in paragraph 4.3 and applying the cumulative mass distribution from Figure 3 gives a fraction of 26% in the t_{3bol} and 32% in the hydrogen-burning shell approximation for white dwarf masses in excess of 0.7 $M_\odot$. Assuming that all ob-

jects with white dwarf masses in excess of 0.7 $M_\odot$ explode as type Ia supernovae after a typical life time of 10^6 years, a SN Ia rate of ∼ $(0.3 - 3) \times 10^{-3}$ yr^{-1} is inferred (in both approximations). Assuming that all objects with white dwarf masses in excess of 0.5 $M_\odot$ explode as type Ia supernovae after a typical life time of 10^6 years (cf. Yungelson et al. 1995), a SN Ia rate of $(0.8 - 7) \times 10^{-3}$ yr^{-1} is inferred (for the two approximations). Supersoft sources could then contribute up to a rate of 7×10^{-3} yr^{-1}. Capellaro (1997) assuming our Galaxy to be a spiral of type Sb or Sc, detected a Type Ia supernova rate of $(2-2.5)\ 10^{-3}$ yr^{-1} which for M31, with is about two times larger mass, means: $(4-5)\ 10^{-3}$ yr^{-1}. It thus seems that the supersoft X-ray sources can make a major contribution to the Type Ia SN rate in M31.

In is interesting to note that the historical supernova SN 1885 (S And) might be a subluminous SN Ia (Chevalier & Plait 1988, Fesen et al. 1998). This supernova is located in the bulge of M31.

7. Conclusions

From the 1991 *ROSAT PSPC* M31 X-ray point source catalog a sample of 26 candidate supersoft sources has been derived using one of the selection criteria $HR1+\sigma HR1 < -0.8$ or $HR1 < 0.9$, $HR2 + \sigma HR2 < -0.1$ and assuming that the observed count rate is in agreement with the expected steady-state luminosity. For these candidates absorbing hydrogen column densities, effective temperatures and white dwarf masses (assuming the sources are on the stability line of atmospheric nuclear burning) are derived. The observed white dwarf mass distribution of supersoft sources in M31 appears to be constrained to masses $M \gtrsim 0.90\ M_\odot$. The whole population of supersoft sources in M31 is estimated accordingly to be at least 1000 and at most 10,000 taking a theoretical white dwarf mass distribution and a double exponential scale height distribution for the gas and the source distribution into account and under the assumption that the observationally derived sample is restricted to white dwarf masses above 0.90 $M_\odot$. This range of a population has to be compared with the range of a population of ∼800-5000 sources as predicted from population synthesis calculations. We find the source population scale height to be ∼300 pc for a scale height for the gas of 150-600 pc. This is consistent with a young stellar population. Assuming a life time as a steadily nuclear burning white dwarf (a supersoft source) of ∼ $10^6\ yr$ and that all supersoft sources with masses in excess of 0.5 $M_\odot$ are progenitors of supernovae of type Ia, a SN Ia rate of ∼ $(0.8 - 7) \times 10^{-3}$ yr^{-1} is inferred for M31 based on these progenitors. Supersoft sources then comprise 20-100% of the SNe Ia progenitors for a total estimated SN Ia rate of $(4 - 5) \times 10^{-3}$ yr^{-1}.

References

Branch D., Livio M., Yungelson L.R., et al., 1995, PASP 107, 1019

Branch D., 1998, ARA&A 36, 17

Braun R., 1991, ApJ 372, 54

Brinks E., & Shane W.W., 1984, A&AS 55, 179

Cappellaro E., Turatto M., Bennetti S., et al., 1993, A&A 273, 383

Cappellaro E., Turatto M., Tsvetkov M., et al., 1997, A&A 322, 431

Chevalier R.A., & Plait P.C., 1988, ApJ 331, L109

Dickey J.M., & Lockman F.J., 1990, ARA&A 28, 215

DiStefano R., & Rappaport S., 1994, ApJ 437, 733

DiStefano R., 1996, Supersoft X-Ray Sources, Lecture Notes in Physics 472, Springer, 193

Ebisawa K., Asai K., Mukai K., et al., 1996, see Greiner 1996, 91

Evans NW., Gyuk G., Turner M.S., et al., 1998, ApJ 501, L45

Fesen R.A., Gerardy C.L., MClin K.M., et al., 1998, ApJ (subm.)

Greiner J., 1996, Supersoft X-Ray Sources, Lecture Notes in Physics 472, Springer, 75

Greiner J., Supper R., & Magnier E.A., 1997, in Supersoft X-Ray Sources, ed. J. Greiner, LNP 472, Springer, 75

Haiman Z., Magnier E.A., Lewin W.H.G., Lester R.R., et al., 1994, A&A 290, 371

Hartmann H.W., & Heise J., 1997, A&A 322, 591

Hasinger G., 1994, Rev.Mod.Astr. 7, 129

Hatano K., Branch D., Fisher A., 1997, ApJ 487, L45

Heise J., van Teeseling A., & Kahabka P., 1994, A&A 288, L45

Iben I.Jr., 1982, ApJ 259, 244

Iben I.Jr., & Tutukov A.V., 1985, ApJS 58, 661

Kahabka P., 1995, A&A 304, 227

Kahbaka P. & Trümper J., 1996, Supersoft ROSAT Sources in the Galaxies. In IAU Symposium No. 165, Compact Stars in Binaries, ed. J. van Paradijs, E.P.J. van den Heuvel & E. Kuulkers, Dordrecht: Kluwer, 425

Kahabka P. & van den Heuvel, 1997, ARA&A 35, 69

Kahabka P., 1998, A&A 332, 189

Li X-D, & van den Heuvel E.P.J., 1997, A&A 322, L9

Livio M., 1996, see Greiner 1996, 183

Magnier E.A., Lewin W.H.G., van Paradijs J., et al., 1992, A&AS 96, 379

Magnier E.A., Prins S., Augusteijn T., et al., 1997, A&A 326, 442

Parmar A.N., Kahabka P., Hartmann H.W., et al., 1997, A&A 323, L33

Parmar A.N., Kahabka P., Hartmann H.W., et al., 1998, A&A 332, 199

Patterson J., Kemp J., Shambrook A., et al., 1998, PASP 110, 380

Sharov A.S., & Alksnis A., 1991, Ap&SS 180, 273

Sharov A.S., & Alksnis A., 1992, Ap&SS 190, 119

Singh K.P., Barrett P., White N.E., et al., 1995, ApJ 455, 456

Supper R., Hasinger G., Pietsch W., et al., 1997, A&A 317, 328

van den Heuvel E.P.J., Bhattacharya D., Nomoto K., & Rappaport S.A., 1992, A&A 262, 97

van Teeseling A., Heise J., & Kahabka P., 1996, in Compact Stars in Binaries, IAU Symposium 165, ed. J. van Paradijs, E.P.J. van den Heuvel, and E. Kuulkers, Kluwer, 445

Walterbos R.A.M., & Kennicutt R.C., 1988, A&A 198, 61

Yungelson L.R., Livio M., Tutukov A., et al., 1995, ApJ 447, 656

Yungelson L.R., Livio M., Truran J.W., et al., 1996, ApJ 466, 890

Yungelson L.R., Livio M., Tutukov A., 1997, ApJ 481, 127

Yungelson L.R., Livio M., 1998, ApJ 497, 168